Journal of Hydrology 652 (2025) 132651

Contents lists available at ScienceDirect

Journal of Hydrology

journal homepage: www.elsevier.com/locate/jhydrol

Research papers

Evolution of pore structure and flow properties in particle segregation

Shaoheng Dai [a], Feng Shan [b], Haibin Xiong [a], Sheng Zhang [b,c], Xuzhen He [a,*], Daichao Sheng [a]

[a] School of Civil and Environmental Engineering, University of Technology Sydney, Ultimo, NSW 2007, Australia
[b] School of Civil Engineering, Central South University, Changsha, 410075, China
[c] School of Civil Engineering, Qinghai University, Xining, 810016, China

ARTICLE INFO

Keywords:
Particle segregation
Pore structure
Lattice Boltzmann Method (LBM)
Discrete Element Method (DEM)
Permeability
Granular materials

ABSTRACT

The Brazil Nut Effect is widely observed in both everyday life and industrial processes. Although extensive research on segregation behaviour, the resulting changes in pore structure and flow properties remain inadequately explored. During particle segregation, the granular system evolves continuously, forming a complex porous media. Understanding the impact of this evolving porous media on fluid transport is crucial across various disciplines. In this study, the Discrete Element Method (DEM) is proposed to analyse the segregation process of granular materials, and the Lattice Boltzmann Method (LBM) is employed to investigate the influence of segregation on macroscopic and microscopic flow properties. The results indicate that particle segregation initially develops rapidly and gradually stabilises, with the evolving contact information illustrating the anisotropy of the granular system. Energy analysis reveals that segregation primarily occurs when the granular material contacts the base. Pore structure analysis shows that pore diameters follow a lognormal distribution, while throat diameters exhibit a bimodal distribution, and sphericity displays a trimodal distribution. As the degree of segregation increases, the top layer experiences a rise in large particles, resulting in higher sphericity and a reduction in pore spaces. Conversely, in the bottom layer, the aggregation of small particles results in lower sphericity and a greater number of pores. Particle segregation induces anisotropic behaviour in the permeability of porous media, with a significant increase in the horizontal direction and a slight decrease in the vertical direction. The tortuosity of the porous media decreases noticeably in the horizontal direction, while exhibiting minimal variation in the vertical direction. These findings underscore the influence of segregation on the pore structure and flow properties of porous media, highlighting the necessity of understanding particle segregation in granular mechanics.

1. Introduction

Granular material refers to aggregates of solid particles (He et al. 2019a; He et al. 2019b; Liu et al. 2022). In a static state, it behaves similarly to a solid, maintaining a defined shape, possessing a specific volume, and withstanding shear forces (Nguyen et al. 2021). Conversely, in a dynamic state, it mirrors fluidic behaviour, allowing for free flow, as observed in events like landslides and debris flows (Bui and Nguyen 2021; He et al. 2018). Moreover, Granular materials can undergo solid-to-liquid phase transitions under external energy inputs, exemplified by liquefaction in sandy soils (El-Sekelly et al. 2016; Wang et al. 2019). Granular materials are therefore extremely complex and interesting. They widely exist in both daily life and industrial processes. Naturally occurring examples include stones, coal, and gravel, while they are also found in consumables such as grains and fruits. Consequently, handling significant amounts of granular materials holds crucial significance in various production processes (Dai et al. 2022; Gao et al. 2022; Muresan et al. 2011; Wu et al. 2017).

In recent years, the Brazil Nut Effect has attracted significant attention in the scientific literature (Dai et al. 2024; Metzger et al. 2011). In simple terms, this phenomenon occurs when a mixture of nuts of different sizes is subjected to vibrations, resulting in the largest nuts rising to the top. While initially observed with nuts, this effect extends to a broad range of granular mixtures. Researchers have been intrigued by the behaviour of shaken granular mixtures, which seemingly defies physical expectations. Despite the bottom of the container being in a more energetically favourable position, larger particles ascend to the surface. Beyond its widespread occurrence in nature, the Brazil Nut

* Corresponding author.
E-mail addresses: shaoheng.dai@student.uts.edu.au (S. Dai), shanfeng1993@126.com (F. Shan), haibin.xiong@student.uts.edu.au (H. Xiong), zhang-sheng@csu.edu.cn (S. Zhang), xuzhen.he@uts.edu.au (X. He), Daichao.Sheng@uts.edu.au (D. Sheng).

https://doi.org/10.1016/j.jhydrol.2024.132651
Received 27 October 2024; Received in revised form 17 December 2024; Accepted 24 December 2024
Available online 3 January 2025

Effect poses challenges in industrial processes. Recent studies on size segregation in rotating drums (Brandao et al. 2020), shear units (Cui et al. 2021), and inclined chute flows (Panda and Tan 2020) have revealed significant separation patterns. The Brazil Nut Effect observed during the transportation and storage of coal further underscores its industrial impact (Li et al. 2022; Liu et al. 2024). Achieving uniform mixtures is essential in most industrial processes, but differences in particle properties can lead to segregation processes, potentially causing stratification of particle beds and significantly affecting the macro–micro properties. As this phenomenon gains increasing attention in contemporary industrial applications, a deeper understanding of its mechanisms and consequences becomes imperative. Experiments indicate that the detailed behaviour of particle size separation, especially in binary mixtures, appears highly complex (Bi et al. 2016). Granular material properties and vibration parameters, such as diameter, friction coefficient, vibrational frequency, and dimensionless acceleration ($\Gamma = A(2\pi f)^2/g$), are generally recognised as the main influencing factors (Dai et al. 2024; Panda and Tan 2020; Qiao et al. 2021). The details and parameter combinations contributing to the Brazil Nut Effect are still under discussion. However, most current research on particle segregation primarily focuses on segregation behaviour and mechanism explanations (Siman-Tov and Brodsky 2018). The consequences of segregation, including the evolution of pore structure and corresponding changes in flow properties, are still poorly understood.

Owing to the unique behaviour of particles in the segregation process, the porous media shaped by the granular system evolves continuously. Its microscopic structure and topological features exhibit a complex formation, characterised by interconnected irregular pore networks presenting a variety of shapes and sizes. Understanding the influence of pore structure on fluid transport is critical for various industrial and environmental processes, spanning disciplines such as geology, engineering, chemistry, and physics. This comprehension holds substantial applications in catalysis, separation and filtration, and the migration of soil pollutants (Bertels and Willems 2023; Chen et al. 2024; Dai et al. 2023). The underlying principles of these processes rely on the flow of fluids through porous materials. For any of these processes, modelling or predicting the impact of pore structure on flow properties becomes essential. However, it is necessary to note that the pore structure is not static, especially in the Brazil Nut segregation process. Consequently, a dynamic comprehension of the pore structure and flow properties of granular systems becomes imperative, and our current knowledge in this area remains limited.

Porous media, particularly natural formations like rocks and soils, represent a diverse category of complex systems. Their pore spaces exhibit significant disorder, featuring a broad range of pore size variations (Chen et al. 2023; Zhang et al. 2024). The complexity of porous media emerges not only from the extensive range of pore sizes but also from the tortuous paths they offer for fluid flow, which deviate from strict linearity to encompass branching, meandering, and interconnected configurations (Feng et al. 2020b; Zhang et al. 2020). As clarified and examined in earlier studies (Sobieski and Lipiński 2019; Song et al. 2022), the flow paths of fluid are often considerably longer than the minimum distance between their initial and final points. During fluid flow through porous media, a complex multiscale phenomenon unfolds, characterised by varying shapes and lengths of flow paths. Tortuosity stands out as a key parameter providing a detailed description of the intricate microstructure within porous media. It plays a critical role in influencing macroscopic flow characteristics, primarily signifying the extent of fluid flow impeded by porous media. Due to the intricate morphology of pore spaces, modelling the pore scale, as well as the flow and transport processes within porous media, is considered a highly complex task. Tortuosity, serving as a bridge between macroscopic infiltration or diffusion processes and the microscopic spatial structure of porous media (Masís-Meléndez et al. 2014; Wu et al. 2018), plays a unique and irreplaceable role. Therefore, understanding the variations in tortuosity is particularly important and necessary for designing and optimising the structure of porous media or comprehending flow.

Segregation significantly impacts the physical properties of granular mixtures, including pore structure and permeability, which describe fluid flow, along with tortuosity, representing the degree of winding and twisting as the fluid passes through porous media. While it is acknowledged that macroscopic properties of granular mixtures may exhibit heterogeneity and anisotropy due to particle segregation, this phenomenon remains unresolved. Hence, in this study, our interest lies in understanding *how the characteristics of granular mixtures, such as pore structure, permeability, and tortuosity, are influenced by particle segregation and packing.* Our goal is to deepen the understanding of particle segregation—an area that has received limited attention. Therefore, this study establishes a numerical analysis framework for characterising the evolution of pore structure during particle segregation and evaluating its impact on the flow properties of granular materials. The structure of this paper is as follows. Section 2 introduces the methods used in this study, including the setup of the DEM model and the validation of the LBM model. Section 3 provides an overall observation of particle segregation to deepen the understanding of the segregation process and obtain samples at different segregation states for subsequent analysis. The impact of particle segregation on the pore structure, permeability, and tortuosity of the samples is quantitatively analysed in Sections 4, 5, and 6, respectively. Finally, Section 7 summarises the main findings of this study.

2. Methodology

The framework of this study is illustrated in Fig. 1. Initially, we use the DEM model to generate a uniformly mixed binary mixture sample and simulate the Brazil nut segregation. Granular systems exhibiting different degrees of segregation represent typical states in the segregation process. Next, we extract and analyse the distribution of pore characteristics for the samples at different segregation levels. Subsequently, Lattice Boltzmann simulations are performed to model fluid flow in the porous medium of these samples. Finally, based on pore geometry features and flow characteristics, we conducted a comparative analysis of the tortuosity evolution in the granular system. The findings of this research contribute to a fundamental understanding of the Brazil Nut Effect, with a specific focus on aspects of the evolution of pore structure and flow properties. It is worth noting that this study is conducted as a combined investigation and does not consider the effects of fluid interactions on particle segregation. Fluid-solid interactions could have a significant impact on particle segregation and its consequences, making this an important area for further exploration.

2.1. Discrete element method

The DEM is a powerful numerical technique for microscopic analysis, commonly employed in the investigation of various phenomena, including granular flow, segregation, and collisions (Chen et al. 2023; Hazzar et al. 2020). In comparison to experimental methods, DEM provides more detailed information about each individual particle. It is noteworthy that studying particle segregation processes and analysing their microstructural and flow properties through traditional laboratory methods poses significant challenges. These challenges involve not only disturbances to the studied samples but also the intricate cooperation of various complex instruments. Therefore, the DEM is employed to simulate particle segregation within a binary mixture (Cundall and Strack 1979; Nie and Wang 2024; Qiu et al. 2024). In DEM simulations, the translational and rotational motions of each particle are governed by Newton's second law of motion, given by:

$$m_i \frac{d\boldsymbol{v}}{dt} = \sum_j \boldsymbol{F}^{ji} + \boldsymbol{f} \tag{1}$$

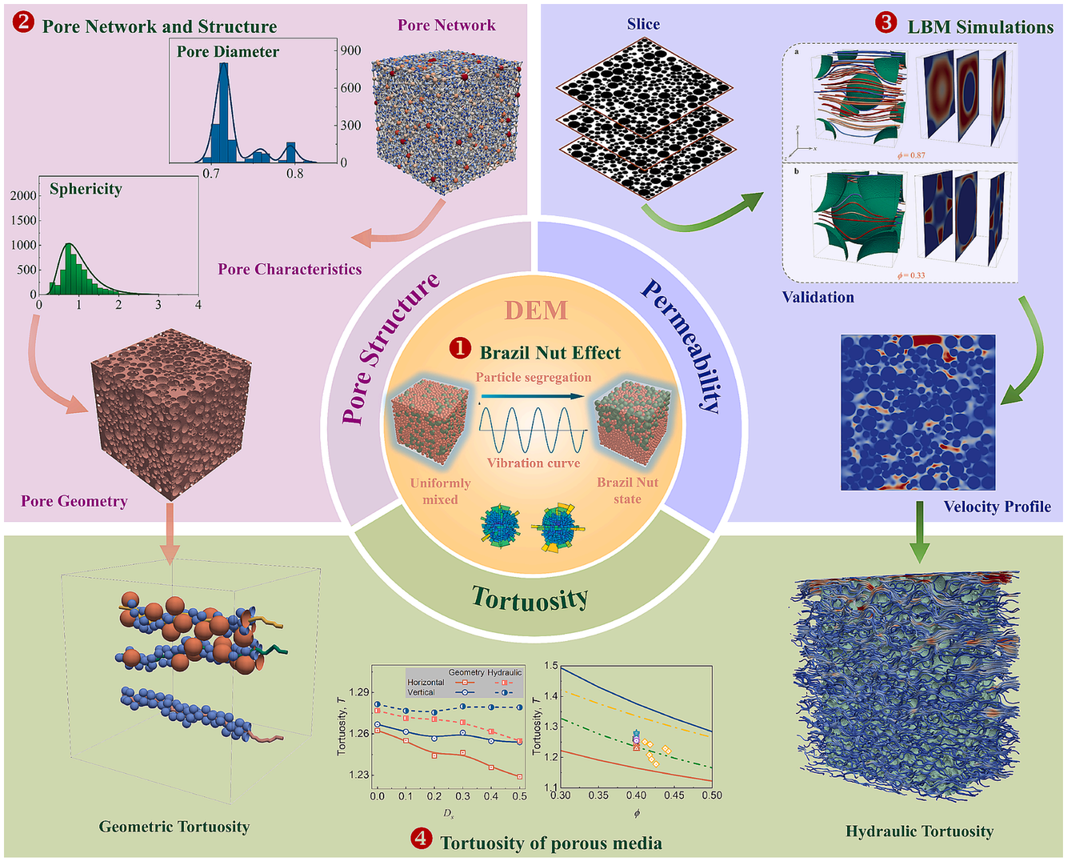

Fig. 1. The framework of this study.

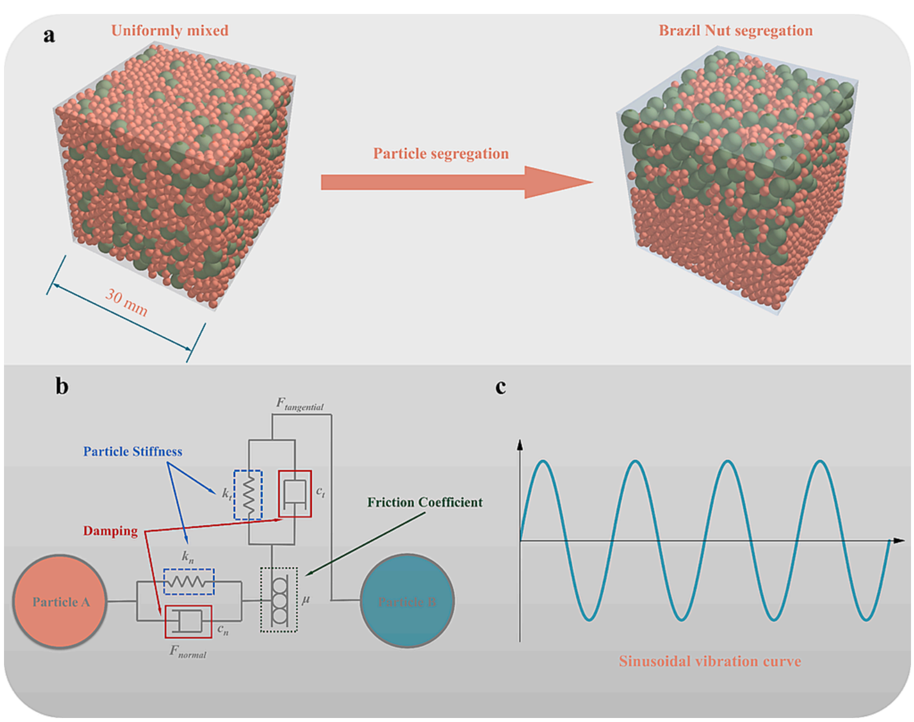

Fig. 2. Simulation settings in the DEM: (a) bed of binary spherical particles; (b) Hertz-Mindlin contact model; (c) vibration curve.

$$I_i \frac{d\omega}{dt} = \sum_j \boldsymbol{T} \tag{2}$$

where $\boldsymbol{v}$ and ω are the translational and angular velocities of the considered particle, respectively; m_i and I_i are the mass and the moment of inertia of particle i, respectively; $\boldsymbol{F}^{ji}$ represents the contact force

Table 1
Main parameters utilised in DEM simulations.

Parameter	Value
Diameter of large particles, D (mm)	3
Diameter of small particles, d (mm)	1.5
Poisson's ratio, ν	0.25
Young's Modulus, E (GPa)	1.0
Coefficient of restitution, e	0.1
Coefficient of static friction, μ_s	0.7
Coefficient of rolling friction, μ_r	0.01
Vibration intensity, Γ	2
Number of large particles, N_L	565
Number of small particles, N_S	4648
Porosity, n	0.4
Density of particles, ρ (g/cm^3)	2600

applied on particle i by particle j; $\boldsymbol{f}$ represents the resultant of the body force; $\boldsymbol{T}$ represents the torque acting on the particle by its neighbouring particles or walls.

Fig. 2 depicts the simulation setup, where the specimen comprises a binary mixture of spherical particles initially arranged in a cubic structure with a side length of 30 mm. A mixture with an initial porosity of 0.4 is generated, comprising large particles (3 mm in diameter) and small particles (1.5 mm in diameter), uniformly mixed in an equal volume ratio. It is important to note that particle shape can influence segregation, and real granular materials often exhibit irregular shapes. Nevertheless, spherical particles, as the most representative form, are used in this study to provide some insights into particle segregation mechanisms. In this study, the container size is approximately 13.3 times the median particle size, ensuring minimal boundary effects and comprehensive capture of local particle behaviour (Guo and Zhao 2013; He et al. 2020). Sinusoidal vertical vibrations are applied to the bottom wall, controlled by $Z = A\sin(2\pi ft)$, where the harmonic motion is characterised by amplitude (A), vibration frequency (f), and time (t). Although various experiments have examined the influence of these factors (Qiao et al. 2021), our primary focus in this study is not their impact. Thus, a vibration amplitude of 1.266 mm and a frequency of 20 Hz were applied, corresponding to a dimensionless vibration intensity of $\Gamma = 2$. Under the influence of the vibration field, the granular system undergoes Brazil Nut segregation, causing large particles to rise to the top. In this work, the conventional Hertz-Mindlin contact model is used to compute the interparticle forces (Hertz 1882; Mindlin 1949). Fig. 2b outlines the basic principles of the Hertz-Mindlin contact model, which is widely utilised for particle contact modelling in granular materials and is proven to be highly successful (Amirifar et al. 2021). Table 1 summarises the basic parameters of the DEM simulation, primarily based on sand parameters previously calibrated and utilised for numerical studies of spherical particle packing (Dai et al. 2024; Feng et al. 2020a; Qiao et al. 2021). To investigate the segregation induced by particle size variation, all particles in the DEM model share identical properties except for differences in size.

2.2. Lattice Boltzmann method

Lattice Boltzmann simulation is conducted using Palabos (Latt et al. 2021), which is renowned for its high flexibility and parallelism, enabling the handling of diverse fluid dynamics problems. The LBM represents fluid as a discrete set of particles moving between nodes along grid lines, following specific rules of streaming and collision until convergence conditions or a specified number of time steps are reached. Extensive discussions on LBM can be found in the literature (Stipić et al. 2022; Wang et al. 2023; Yin et al. 2022; Younes et al. 2023). In this study, flow simulations are conducted on the porous media structure obtained by DEM. The walls of the porous media are treated as reflective boundary conditions. The lattice model employed here is suitable for 3D and consists of 19 discrete velocities, known as D3Q19, as depicted in Fig. 3 (Ding and Xu 2018; Indraratna et al. 2021; Yang et al. 2019). The domain is segmented into cubic cells, each with a set of probability distribution functions f_i, which represent the density of fluid particles passing through each of the 19 discrete velocities. The fluid particle density at a specific position within the lattice is calculated using the following expression:

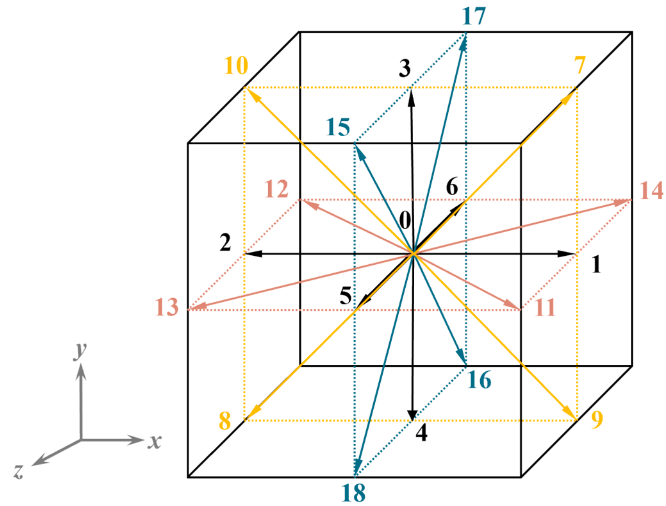

Fig. 3. A D3Q19 lattice structure for LBM simulations.

$$\rho(\vec{\mathbf{x}}) = \sum_{i=0}^{19} f_i(\vec{\mathbf{x}}) \tag{3}$$

where, $\vec{\mathbf{x}}$ refers to the position of the cell, specifically at its centre.

The velocity corresponding to each cell position can be defined by:

$$\vec{\mathbf{u}}(\vec{\mathbf{x}}) = \frac{\sum_{i=0}^{19} f_i(\vec{\mathbf{x}})\vec{\mathbf{e}}_i}{\rho(\vec{\mathbf{x}})} \tag{3}$$

where, $\vec{\mathbf{e}}_i$ denotes the i-th discrete velocity (with i ranging from 0 to 19). The D3Q19 set of discrete velocities can be expressed in matrix form as follows:

$$E = \begin{bmatrix} 0 & 1 & -1 & 0 & 0 & 0 & 0 & 1 & -1 & 1 & -1 & 1 & -1 & 1 & -1 & 0 & 0 & 0 & 0 \\ 0 & 0 & 0 & 1 & -1 & 0 & 0 & 1 & -1 & -1 & 1 & 0 & 0 & 0 & 0 & 1 & -1 & 1 & -1 \\ 0 & 0 & 0 & 0 & 0 & 1 & -1 & 0 & 0 & 0 & 0 & 1 & -1 & -1 & 1 & 1 & -1 & -1 & 1 \end{bmatrix} \tag{4}$$

The velocity along each direction is described by:

$$|\mathbf{e}_i| = \begin{cases} 0i = 0 \\ 1 \bullet ci = 1, 2, 3 \cdots 6 \\ \sqrt{2} \bullet ci = 7, 8, 9 \cdots 18 \end{cases} \tag{5}$$

where, $c = \delta_x/\delta_t$ represents the characteristic lattice velocity, which is determined by the grid spacing δ_x and the time step δ_t. The weight factors of the D3Q19 lattice are given by:

$$\omega_i = \begin{cases} \frac{1}{3} i = 0 \\ \frac{1}{18} i = 1, 2, 3 \cdots 6 \\ \frac{1}{36} i = 7, 8, 9 \cdots 18 \end{cases} \quad (6)$$

At each time step, the particles at all nodes move along their respective directions to adjacent nodes, undergo collisions, and form new particle distributions. The change in density distribution before and after collisions is typically calculated using a single-relaxation time approximation. Thus, in computation, each time step involves two operations: streaming and collision. The streaming operation is expressed as:

$$f'(\mathbf{x} + \mathbf{e}_i\delta_t, t + \delta_t) = f_i(\mathbf{x}, t) \quad (7)$$

The collision operation is expressed as:

$$f_i(\mathbf{x} + \mathbf{e}_i\delta_t, t + \delta_t) = f'(\mathbf{x} + \mathbf{e}_i\delta_t, t + \delta_t) - \frac{\left[f_i(\mathbf{x}, t) - f_i^{eq}(\mathbf{x}, t)\right]}{\tau} \quad (8)$$

Here, τ denotes the dimensionless relaxation time, and f_i^{eq} refers to the equilibrium distribution functions, which are dependent on the macroscopic variables, density (ρ) and velocity ($\boldsymbol{u}$) at position x and time t.

These two operations can be unified as follows:

$$f_i(\mathbf{x} + \mathbf{e}_i\delta_t, t + \delta_t) - f_i(\mathbf{x}, t) = -\frac{\left[f_i(\mathbf{x}, t) - f_i^{eq}(\mathbf{x}, t)\right]}{\tau} \quad (9)$$

For the D3Q19 model, the equilibrium functions are:

$$f_i^{eq}(\mathbf{x}, t) = \omega_i\rho(\mathbf{x})\left(1 + 3\frac{\vec{\mathbf{e}}_i \bullet \vec{\mathbf{u}}}{{c_s}^2} + 9\frac{(\vec{\mathbf{e}}_i \bullet \vec{\mathbf{u}})^2}{2{c_s}^4} - \frac{3\mathbf{u}^2}{2{c_s}^2}\right) \quad (9)$$

To validate the accuracy of the LBM program, simulations are conducted to validate the pressure-driven flow in Body-Cantered Cubic (BCC) arrays. The LBM domain consists of 200x200x200 cells, with periodic boundary conditions applied on the sides. No-slip bounce-back boundary conditions were used on the surface of obstacles, and pressure conditions were set at the inlet and outlet. The fluid density is $\rho = 1000$ kg/m^3, and the kinematic viscosity is $\mu = 1.01 \times 10^{-3}$ Pa·s. Fig. 4 presents the results for BCC arrays with porosities of 0.87 and 0.33, showing flow paths and velocity profiles.

Based on the Kozeny-Carman equation (Carman 1956; Kozeny 1927), the permeability of porous media composed of spherical particles can be expressed as:

$$K = \frac{A\phi^3}{(1-\phi)^2}, A = \frac{D_p^2}{180} \quad (10)$$

where, ϕ is the porosity. D_p is the diameter of the volume equivalent spherical particle.

More in-depth research has been conducted on the permeability of BCC structures (Eshghinejadfard et al. 2016; Sangani and Acrivos 1982), and a comparison of the results obtained from these studies is presented in Fig. 5. The findings show a good agreement between the simulations conducted in this study and the relevant data. However, it is essential to note that some differences are observed, particularly when the porosity is either small or large. Within the porosity range studied in our

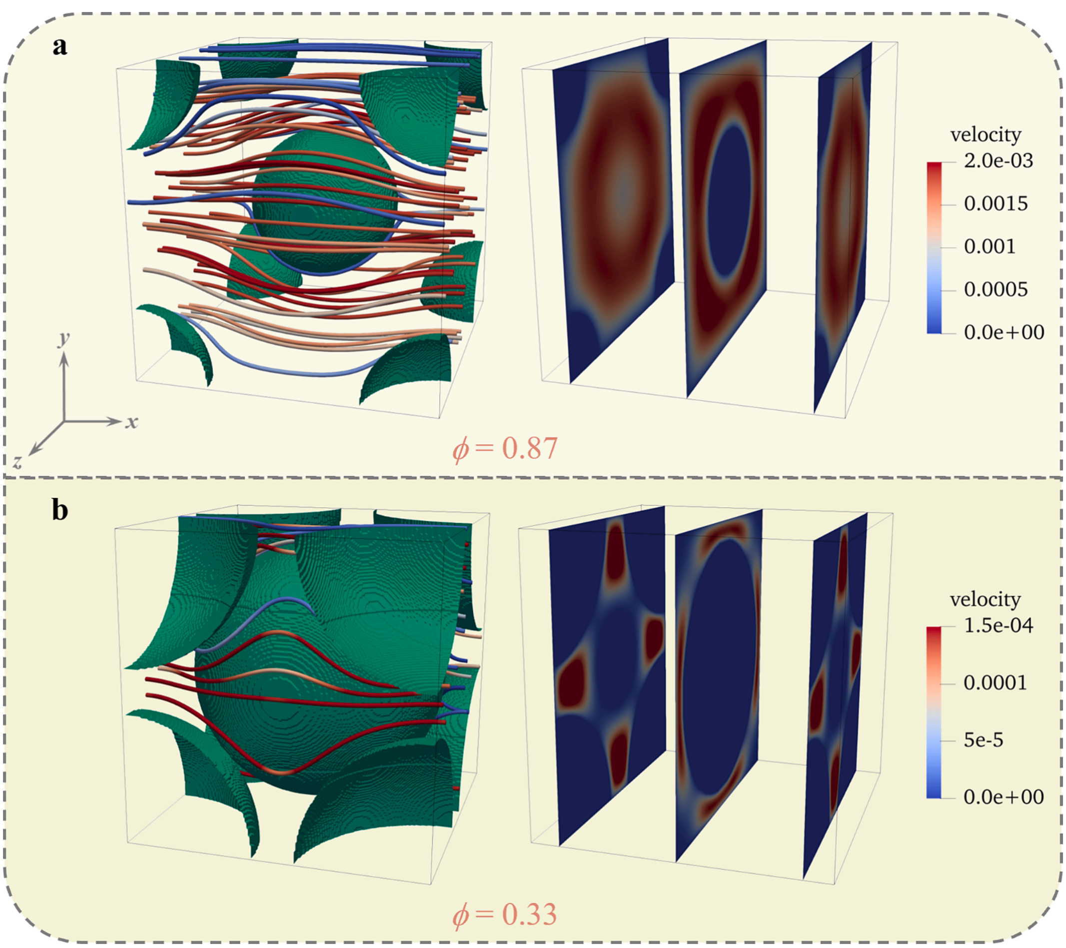

Fig. 4. Flow simulation in BCC arrays, with the porosity of (a) 0.87, and (b) 0.33.

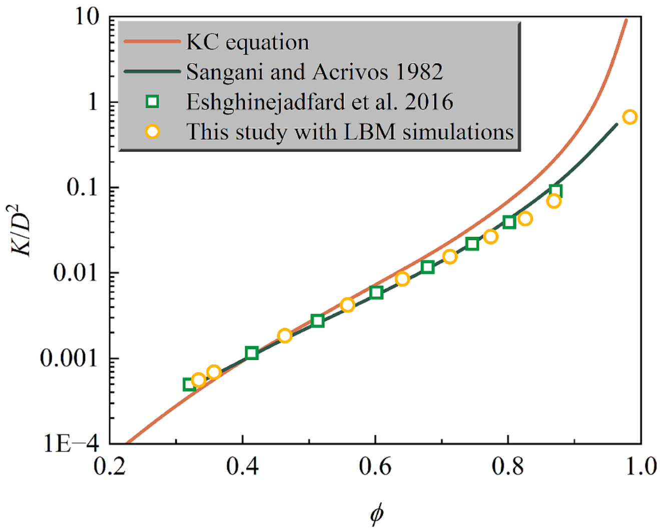

Fig. 5. Comparison of the results of the simulation and the literature (Eshghinejadfard et al. 2016; Sangani and Acrivos 1982).

research, the model presented in this paper can be considered reliable.

3. Particle segregation observation

Under the influence of the vibration field, initially uniformly mixed granular systems undergo Brazil Nut segregation, resulting in large particles rising while small particles descend, forming a layered granular system. Fig. 6 illustrates the segregation evolution of the binary mixture subjected to vertical vibration. The graph depicts the segregation index (D_s) and the normalised average height as functions of vibration cycles. Here, D_s is defined as the degree of segregation, given by:

$$D_s = 2\frac{h_l - h_s}{h_l + h_s} \tag{11}$$

Where, h_p is the average height of particles of species $p = l; s$ ($h_p = (1/N_p)\sum_{i=1}^{N_p} z_i$), here z_i denotes the height of particle i relative to the container base.

From Fig. 6, it is evident that initially, the large and small particles are uniformly mixed, and their average heights are approximately 0.5, resulting in a segregation index of 0. After 260 vibration cycles, the average height of the large particles increases from 0.5 to 0.64, while the small particles decrease from 0.5 to 0.39. That means faster separation of large particles. Visual observation of the segregated granular system reveals that some small particles remain retained at the upper part. This is believed to be related to the migration and clogging process of fine particles. The development of the segregation index also indicates that the process undergoes rapid development in the initial stages, and gradually slows down until reaching a stabilised state. In this study, the granular system does not reach fully Brazil Nut segregation (the final D_s = 0.52) even after 260 vibration cycles. The stable limit that particle segregation can reach is considered to be influenced by various factors, such as the particle diameter ratio, friction coefficient, vibration intensity, etc. (Metzger et al. 2011). However, these factors are not the focus of this research and will not be discussed further.

The granular system undergoes a continuous evolution from a uniformly mixed state to a Brazil Nut segregation state, constantly rearranging particles to form new packing configurations and fabrics. The contact between particles plays a crucial role in the internal force transmission of the granular system. In this work, the binary mixture system is categorised into large-large particle contacts (L-L), small–small particle contacts (S-S), and large-small particle contacts (L-S) based on their contact types. Fig. 7(a) illustrates the variation in the number of different contact types with the degree of segregation. It can be observed that as segregation occurs, large particles gather at the upper part of the system, leading to a slight increase in the number of L-L contacts. Similarly, small particles accumulate at the lower part, resulting in a continuous increase in the number of S-S contacts. On the other hand, the contacts between large and small particles steadily decrease, indicating the segregation process. Fig. 7(b) shows the rose diagrams illustrating the directions of normal contact. In the initial sample, the number of contacts is evenly distributed in spatial direction. As segregation develops, the contacts initially become concentrated in the vertical direction, followed by an increase in the horizontal direction, ultimately forming an anisotropic distribution. These differences result from the spatial structural evolution caused by particle segregation. It is important to note that sufficient contact (coordination number) is necessary to maintain particle stability in three-dimensional space. During segregation, particles intermittently contact and separate. To et al. (2016) found that a contact number below a certain threshold indicates particle instability, which may be related to the mechanisms of particle segregation. The study of contact behaviour is both intriguing and valuable, warranting further exploration.

Energy analysis of the granular system is essential for a comprehensive understanding of particle interactions and the segregation process, as depicted in Fig. 8. The potential energy (E_P), with respect to the centre of the container, is defined as:

$$E_P = \sum_{i=1}^{N} m_i g h_i \tag{12}$$

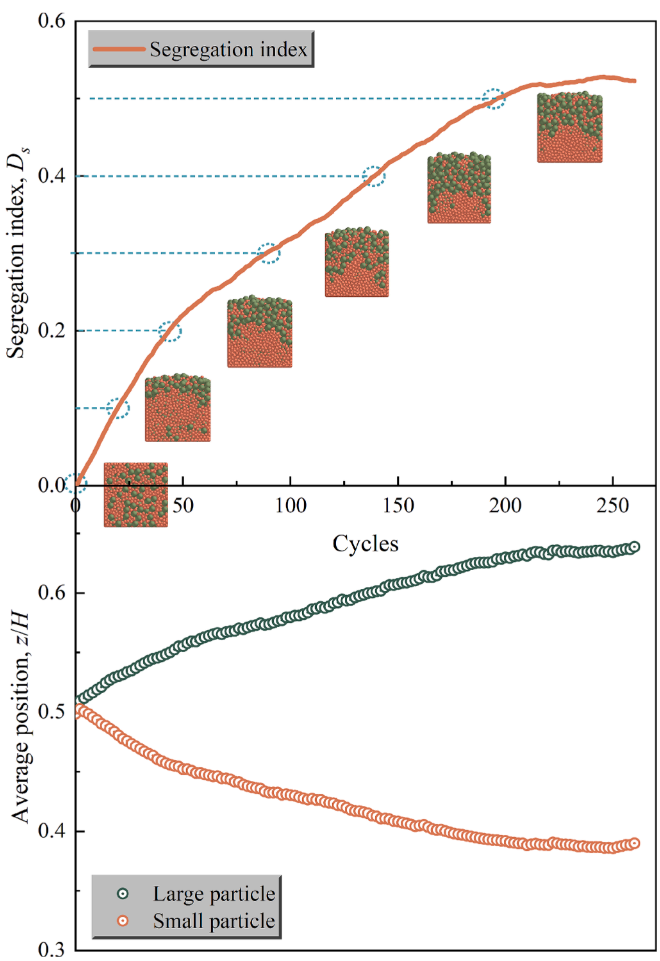

Fig. 6. Segregation evolution with vibration cycles.

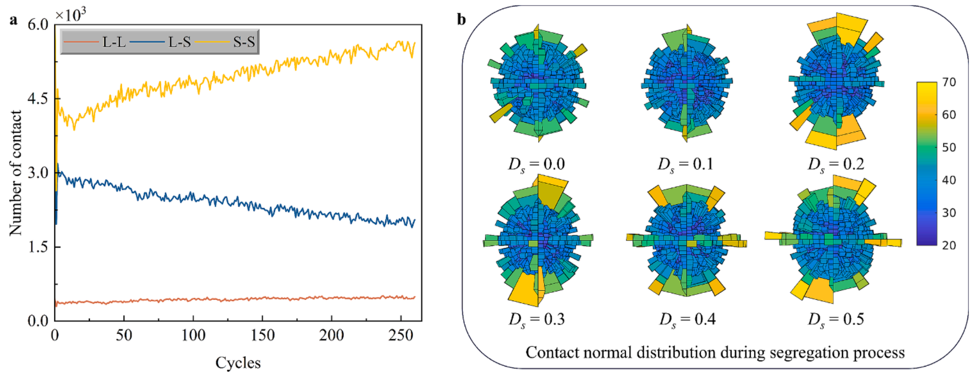

Fig. 7. Contact information of particles: (a) number of contacts; (b) contact normal distribution.

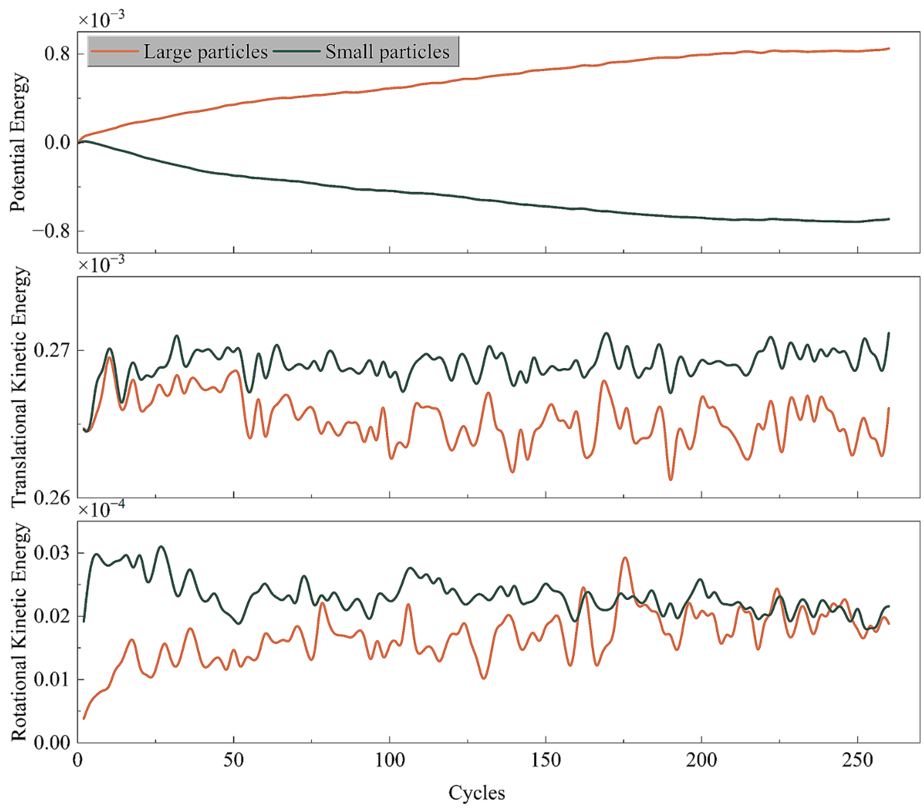

Fig. 8. Energy evolution during segregation.

Here, N is the total number of particles considered; m_i and h_i are the mass and height of particle i, respectively. Before segregation, E_P corresponds to the system's total energy (E_0). The kinetic energy (E_K) can be divided into translational kinetic energy (E_{Kt}) and rotational kinetic energy (E_{Kr}), defined as:

$$E_{Kt} = \frac{1}{2}\sum_{i=1}^{N} m_i|v_i|^2 \tag{13}$$

$$E_{Kr} = \frac{1}{2}\sum_{i=1}^{N} I_i|\omega_i|^2 \tag{14}$$

where, $I_i = 0.4 m_i r_i^2$ is the moment of inertia, r_i is the particle radius, and v_i and ω_i are the translational and rotational velocities, respectively.

Fig. 8 reveals that initially, the potential energy of large and small particles is almost the same. However, as segregation occurs, the potential energy of large particles increases, while that of small particles decreases. This trend aligns with the change in the average height of particles shown in Fig. 6. In the initial stage, when large and small particles are uniformly mixed, the granular system behaves as a collective entity under the influence of the vibrational field. Consequently, at this stage, the translational kinetic energy between large and small particles undergoes relatively consistent changes. At the onset of segregation, the difference in translational motion between large and small particles is minimal, while rotational kinetic energy exhibits the largest difference. As segregation progresses and the granular system changes, the difference in translational kinetic energy between large and small particles becomes more noticeable. Large particles rise to the top, gaining more freedom of movement, especially in areas where they are more loosely packed, making it easier for them to rotate. In contrast, small particles move to the bottom, where their ability to rotate is more limited.

Fig. 9(a), (b), and (c) respectively show the evolution of potential energy, translational kinetic energy, and rotational kinetic energy over

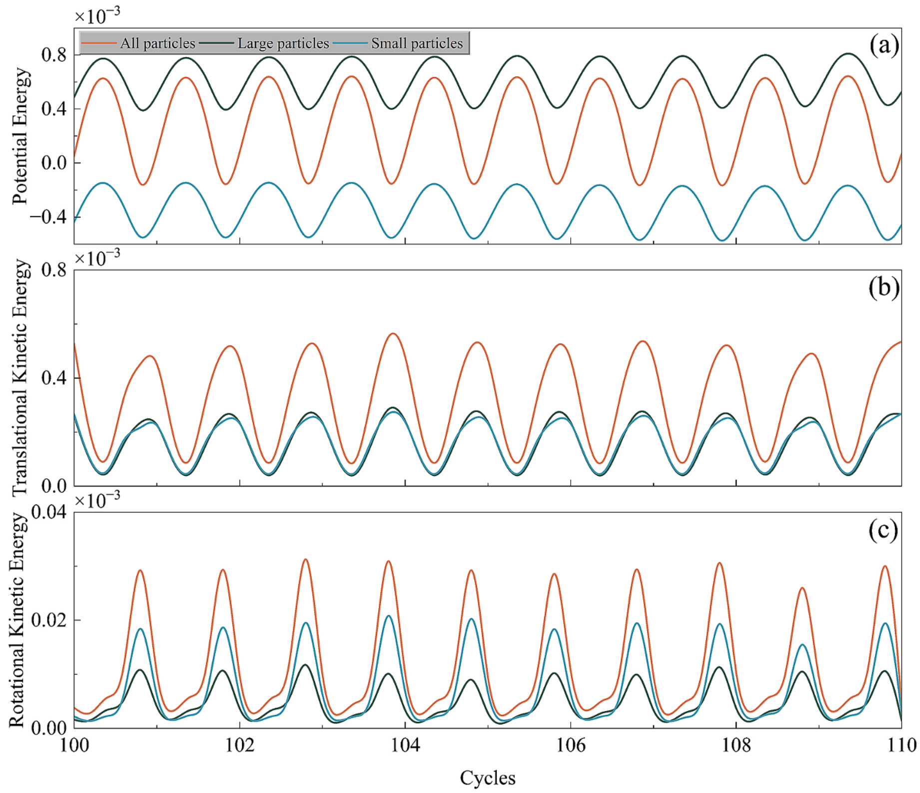

Fig. 9. Evolution of (a) potential energy, (b) translational kinetic energy, and (c) rotational kinetic energy during ten local sequential cycles.

ten local sequential cycles during segregation (note that the vertical axis scale in Fig. 9 differs from that in Fig. 8). The overall granular system undergoes sinusoidal motion with the vibrational field, resulting in a sinusoidal trend in potential energy. The energy input from the bottom vibrating plate is transient. Therefore, within a single cycle, potential and kinetic energies undergo mutual conversion, with kinetic energy exhibiting an approximate cosine variation. The primary motion of the granular system is translational, and rotational kinetic energy is relatively small. Rotational motion among particles mainly occurs during the descent of the granular system when it contacts the bottom plate. During this period, granular system receives energy input from the bottom plate, and the rotational motion is evident due to collisions and contact with the bottom plate. By the 100th cycle, the difference in potential energy between large and small particles becomes apparent, indicating clear particle segregation. The translational kinetic energy of large and small particles remains mostly consistent, diverging only when the granular system contacts the bottom plate. Furthermore, significant differences in rotational kinetic energy have been observed. When large and small particles maintain coordinated motion, there is minimal segregation occurring. Hence, it can be inferred that segregation primarily occurs during the descent phase. During this period, translational and rotational kinetic energies of the granular system undergo significant changes. The continuous relative displacement in each cycle induces motion among particles, leading to alterations in the spatial position and structure of the granular system.

4. Pore structure

The profound impact of pore structure on transport processes is a distinctive characteristic shared by all porous materials. Even among materials with the same porosity, variations in transport characteristics can be substantial, owing to factors such as spatial distribution, connectivity, shape, and size distribution of the pores (Bakhshian et al. 2019; Ishiyama et al. 2023). Due to this significant dependence on pore structure, visualisation emerges as a crucial element in the analysis of porous media (Yamamoto et al. 2023). In this study, the impact of particle segregation on pore characteristics is investigated by extracting the pore network from the porous structure. Pore network extraction is a methodology that models continuous pore structure as localised, isolated pore bodies (pores) and their connecting regions (throats). During this process, each identified subregion corresponds to a pore body within the extracted pore network, and these subregions are interconnected by narrow interfaces, corresponding to throat connections. Various methods, such as the medial axis-based method (Lindquist et al. 1996), maximum ball-based method (Xiong et al. 2022), and watershed segmentation method (Gostick 2017; Zhao et al. 2020), can be employed for extracting the pore network from real porous geometric structures. In this study, the watershed segmentation method is utilised to decompose the porous medium into subregions and to extract the pore network. As depicted in Fig. 10, the watershed method is applied to segment the pore space of the porous medium and reconstruct the pore structure. This methodology has been implemented in the open-source algorithm SNOW (Gostick 2017). Previous research has demonstrated a good level of consistency between statistical size of the pore geometries extracted from experimental and DEM samples.

The pore structure undergoes evolution in the granular system during the segregation process. To quantitatively analyse the differences in the network, a series of parameters are calculated for granular systems at different degrees of segregation, including pore diameters, throat diameters, and sphericity, as illustrated in Fig. 11. Sphericity is an index measuring the spherical nature of pore shapes, defined as:

$$Sphericity = \frac{\pi^{1/3}(6Vol)^{2/3}}{A} \tag{15}$$

where, Vol and A are the volume and surface area of the pores, respectively.

It should be noted that pore networks are different from concepts like constrictions (To et al. 2016b, To et al., 2018, To et al., 2020). They

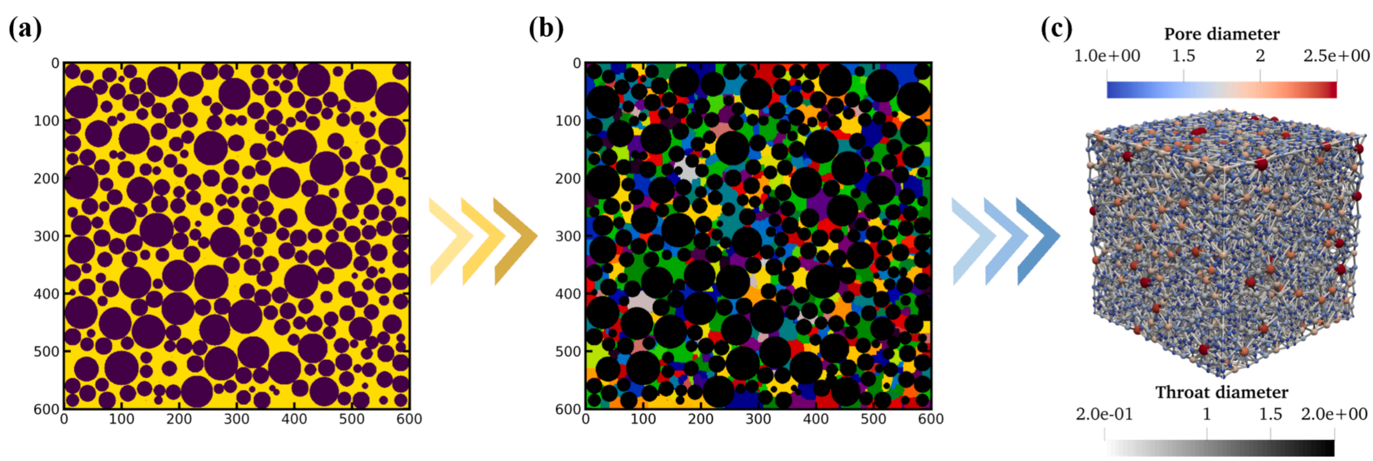

Fig. 10. Reconstruction of the pore structure using the watershed method: (a) packing of granular material; (b)pore extraction, where black indicates the solid matrix, coloured regions represent void pore spaces, and boundaries between coloured regions indicate pore boundaries identified using the watershed method; and (c) final pore networks constructed.

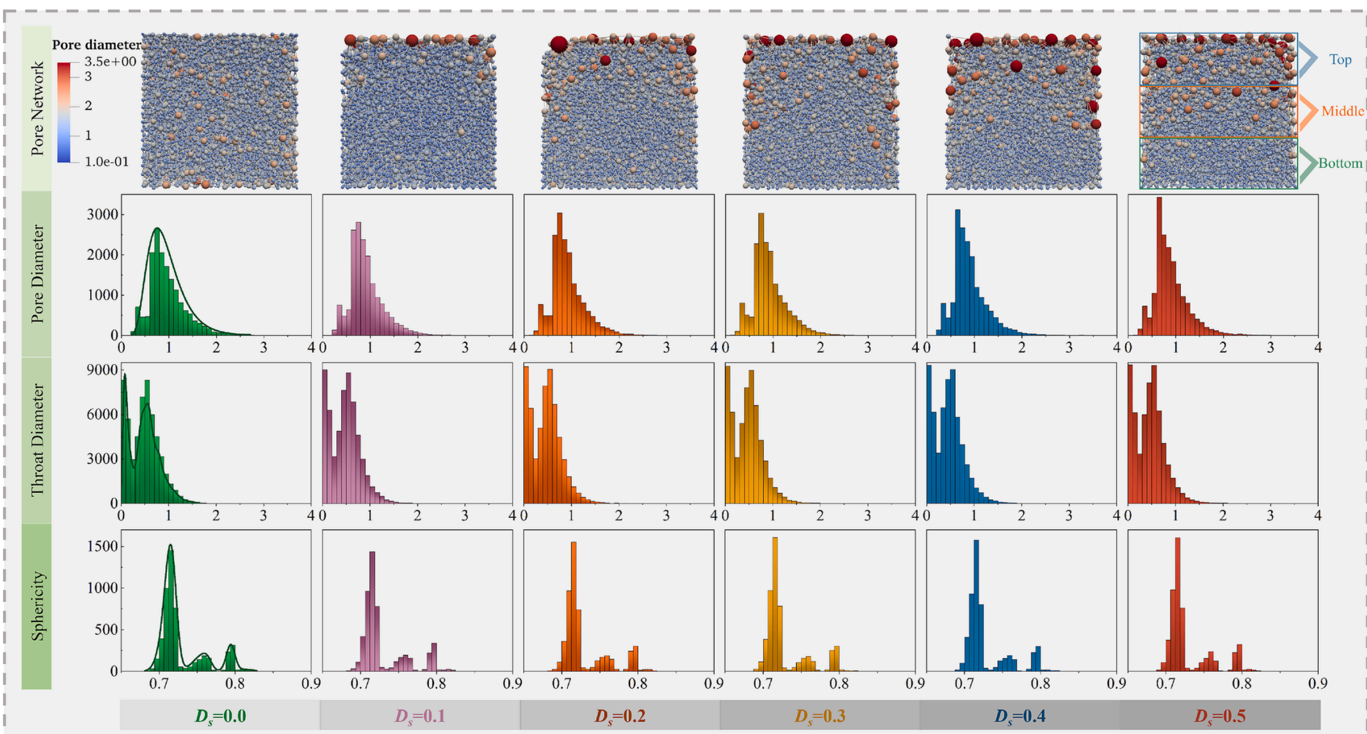

Fig. 11. Evolution of overall pore structure during particle segregation.

primarily rely on precise partitioning of the image space, which remains a significant challenge. In the case of complex pore spaces, the distance transform can show local maxima, potentially leading to over-segmentation and errors in the identification of pores and throats. Moreover, methods based on equivalent volume may overestimate the actual size of pores (To et al. 2012). Despite these limitations, the pore network method still provides valuable insights into the evolution of pore structure during the particle segregation process. The extracted network presented in 1st row of Fig. 11 demonstrates the evolution of the internal pore structure. In the initial granular system, characterised by a uniform distribution of large and small particles, the distribution of pore structures remains relatively even. However, as segregation takes place, large particles accumulate in the upper part. Consequently, their void volumes become relatively larger, and the number of pores and throats decreases. Data statistics reveal that pore diameters roughly follow a lognormal distribution (2nd row in Fig. 11), with an average diameter of approximately 1 mm. Throat diameters, noticeably smaller than pore diameters, exhibit a bimodal distribution. Ren and Santamarina (2018) clarified that the throat radius is approximately half of the pore radius, aligning with the findings of this study. The sphericity of pore structures demonstrates a trimodal distribution, with one dominant peak. As the degree of segregation increases, the evolution of pore structure characteristics is not apparent. This phenomenon is acceptable, as segregation merely prompts particle rearrangement, primarily influencing local structure without substantial alterations to the overall configuration.

Further examination of the local structure evolution, depicted in Fig. 12, illustrates the distribution of pore diameter and sphericity. The structure is subdivided uniformly into top, middle, and bottom sections along the Z-axis for individual statistical analysis. When the segregation

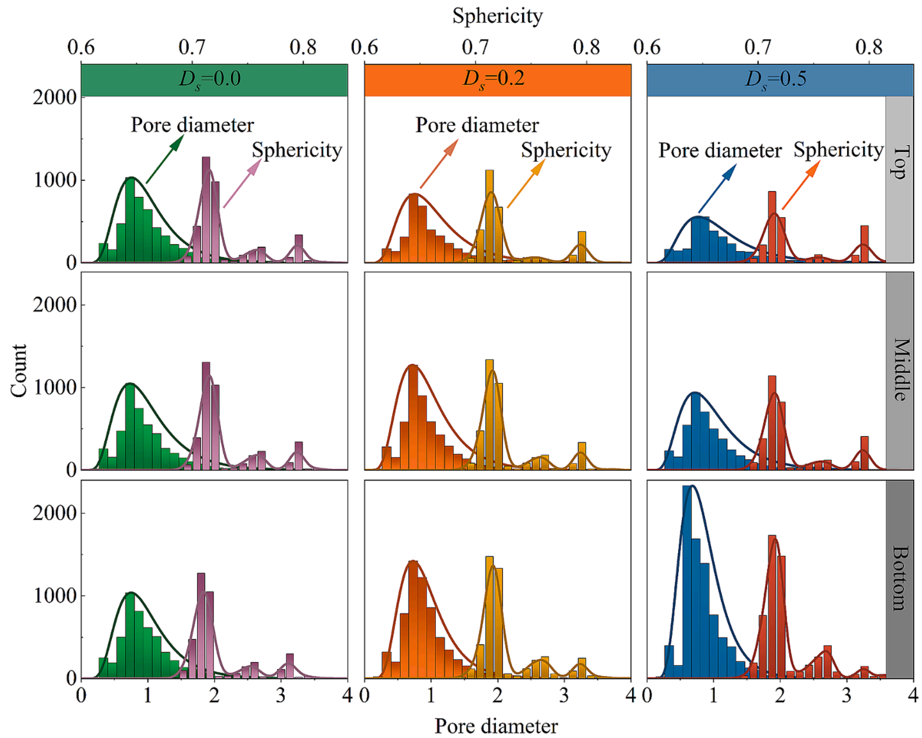

Fig. 12. Evolution of local pore structure during particle segregation.

degree is 0, the granular system exhibits uniform distribution overall, resulting in similar distributions of pore diameter and sphericity across the top, middle, and bottom sections. However, as segregation progresses, large particles tend to aggregate towards the top layer, while small particles aggregate in the bottom layer. This leads to a mixture of large and small particles moving within the middle layer, thereby generating distinct pore structures. In the top layer, the increase of large particles promotes the formation of larger pores, leading to a reduction in pore count while increasing the number of pores exhibiting higher sphericity. Conversely, in the bottom layer, the aggregation of small particles facilitates the formation of intricate smaller pores, thereby increasing the pore count while decreasing the number of pores with higher sphericity. The middle layer represents an intermediate state between the top and bottom layers, demonstrating a slight increase followed by a decrease in pore diameter and sphericity distribution. However, these alterations in the middle layer are minor.

5. Flow properties

Particle segregation causes large particles to aggregate in the upper part of the system, leading to a noticeable increase in pore and throat sizes. Conversely, small particles gather in the lower part, resulting in the opposite effect. The permeability of porous media is believed to be closely related to pore distribution, and with the increase in pore and throat sizes, permeability is expected to rise, and vice versa. In our study, the overall porosity of the porous media remains consistent, but there are localised increases in the upper part and decreases in the lower part. This complexity in pore structure makes predicting overall permeability challenging. Additionally, particle segregation introduces notable anisotropy to the particle distribution, potentially causing variations in both vertical and horizontal flow within the pore space. The pore structure significantly influences the flow within the pore space, posing challenges for the analysis of flow characteristics at both macro and micro scales. Therefore, as depicted in Fig. 13, the flow simulations in vertical and horizontal orientations for porous media are conducted

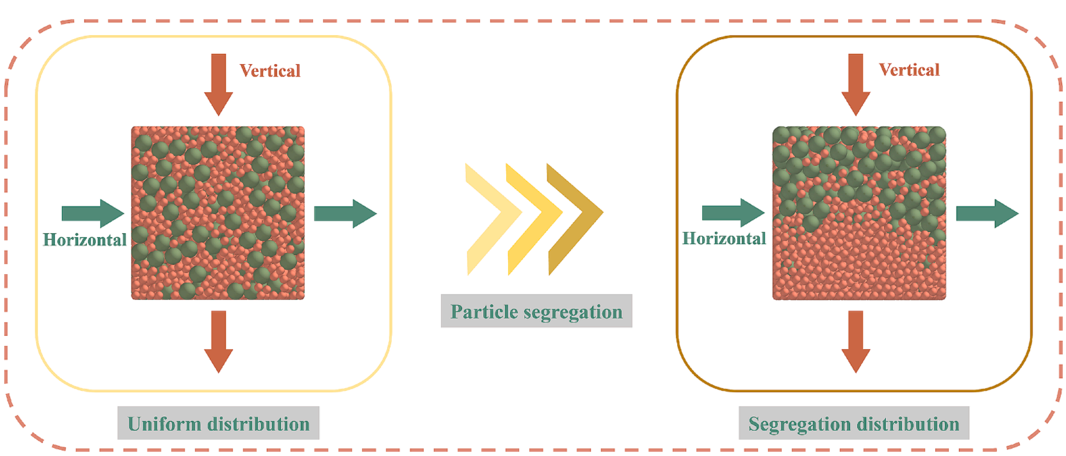

Fig. 13. Scheme of flow simulation.

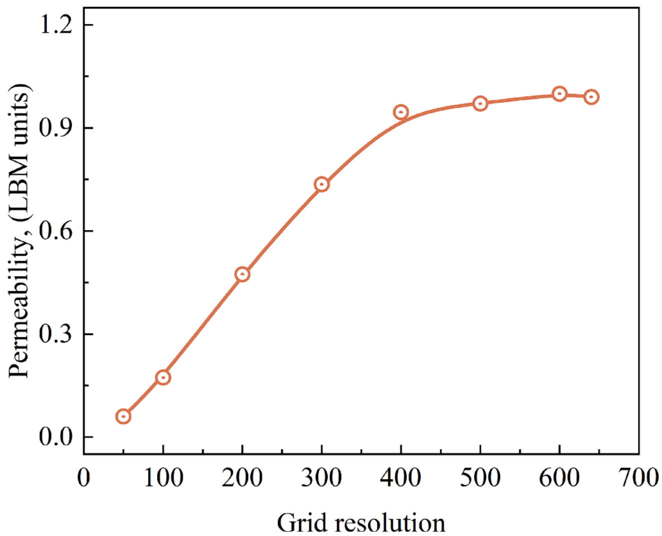

Fig. 14. Permeability evolution for different grid resolutions.

under different states of segregation, aiming to investigate the influence of particle segregation on the anisotropy of flow properties.

In this section, a series of LBM simulations is conducted to investigate fluid flow in porous media at various degrees of segregation. In the simulations presented below, periodic boundaries are employed on the lateral sides, no-slip bounce-back boundary conditions are applied on obstacle surfaces, and pressure conditions are set at the inlet and outlet. Flow characteristics in the pore space under low Reynolds numbers are captured by gradually changing the pressure difference between the inlet and outlet. The relaxation time is set to $\tau = 1$, and the kinematic viscosity is $\nu = 1/6$ (in lattice units). The influence of grid size on computational accuracy is investigated using the uniformly distributed sample ($D_s = 0$), considering their smaller and more complex pore structure. Multiple simulations are performed at different grid resolutions, and the results are presented in Fig. 14. These findings indicate that grid resolution has a notable impact on fluid flow in porous media, with permeability gradually stabilising as the grid becomes finer. While there are slight variations in the simulation results with further refinement, these deviations are considered acceptable. To ensure the stability and reliability of the results, a grid density of 500 × 500 × 500 is used for subsequent porous models in the flow simulations.

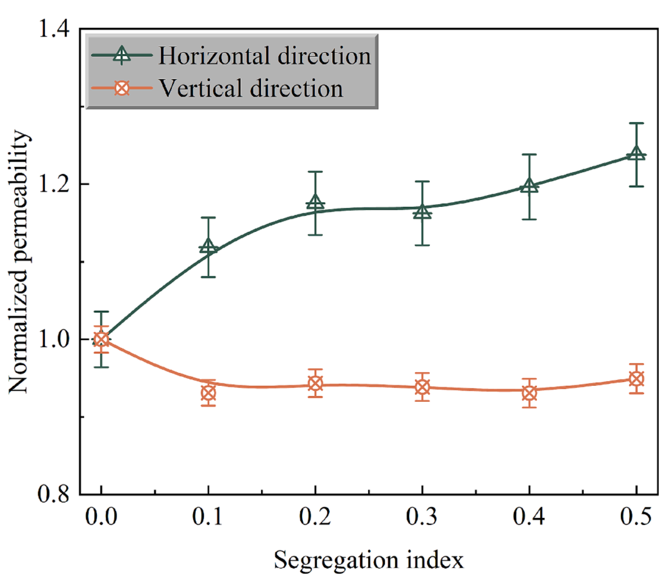

Fig. 15. Permeability results from numerical simulations.

Permeability.

The permeability results of the granular system in both horizontal and vertical directions are presented in Fig. 15, obtained from six repeated simulations conducted at different Reynolds numbers for each sample. Permeability was calculated using Darcy's law, with low Reynolds number laminar flow maintained by controlling the pressure boundary conditions. The simulations were run on an Intel Xeon E-2488G processor (3.2 GHz base frequency), with each LBM simulation taking approximately 12 h, depending on the sample structure and boundary conditions. The results are normalised via the permeability coefficient of the system at $D_s = 0$. It is evident from the results that particle segregation induces an increase in permeability in the horizontal direction, while the permeability in the vertical direction experiences a slight decrease followed by a relatively constant behaviour. As discussed earlier, particle segregation causes large particles to aggregate in the upper layer, leading to increased local porosity in that region. Consequently, during horizontal flow, there is a preferential flow through the porous media towards areas with larger pores, as will be demonstrated in the velocity profile below. In contrast, during vertical flow, the aggregation of small particles in the lower part leads lower local porosity, and overall smaller permeability. Overall, the occurrence of segregation introduces anisotropy in the pore structure, resulting in variations in permeability.

Velocity profile.

The spatial distribution of porous media significantly influences pore flow. Figure 16 illustrates the velocity results during the vertical flow process as porous media evolves with particle segregation, showcasing cross-sections of representative samples. As depicted in Figure 16(b), similar to the evolution of permeability, the fluid almost uniformly flows through the pore space in the flow domain, suggesting that particle segregation has a minimal impact on vertical flow. A more detailed examination of velocity distribution is presented in Figure 16(c, d), revealing higher local velocities near the boundaries (sections I-I and III-III). This phenomenon can be attributed to the combined effects of particle distribution and boundaries.

Fig. 17 illustrates the velocities profile in horizontal flow. The distribution of pores in porous media significantly influences the flow patterns, and the differences in horizontal flow of porous media under different segregation states become more pronounced. As particle segregation occurs, higher velocities are observed in the upper part of the porous media, where the pores and throats are larger, and the reverse is true for the lower part. Additionally, according to Fig. 17(c, d), fluid flowing through large pore pathways (section I-I) obtains higher velocities than fluid flowing through small pore pathways, indicating a preferential flow. This result is consistent with flow through parallel pipes, where, due to lower flow resistance, fluid travels at higher speeds through larger pathways. These findings highlight the significant impact of pore structure evolution due to particle segregation on the anisotropy of porous media permeability.

6. Tortuosity

The complex structure of porous media creates intricate pathways for fluid flow, electrical conduction, and molecular diffusion, all of which significantly impact their transport behaviours. Tortuosity is a key parameter used to describe these properties, encompassing various types such as geometric tortuosity (T_g), hydraulic tortuosity (T_h), electrical tortuosity (T_e), and diffusion tortuosity (T_d). The relative magnitudes of these tortuosities were believed to follow the order $T_g < T_d \approx T_e < T_h$ (Fu et al. 2021; Ghanbarian et al. 2013). However, due to a lack of direct comparisons, these relationships are still unclear. Notably, despite differences in conceptual backgrounds, most tortuosity models are considered functions of porosity. In this study, our focus is specifically on exploring the differences between hydraulic and geometric tortuosity, with the aim of investigating the impact of particle segregation on the tortuosity of porous media.

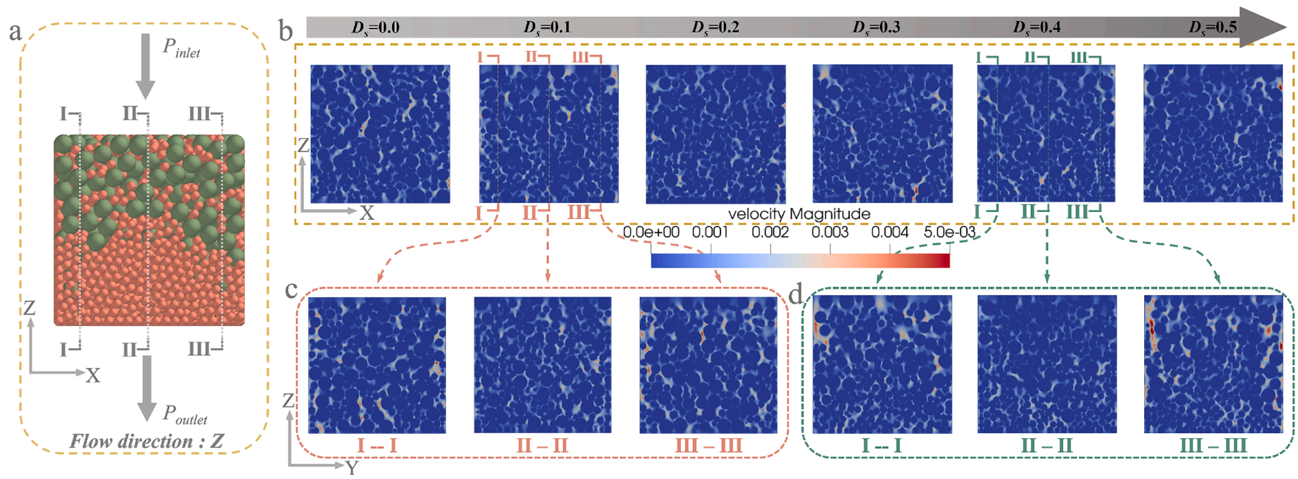

Fig. 16. (a) Schematic diagram of vertical flow, (b) evolution of the velocity profile at the centre section with the degree of segregation, (c) velocity profile with D_s = 0.1, and (d) velocity profile with D_s = 0.4.

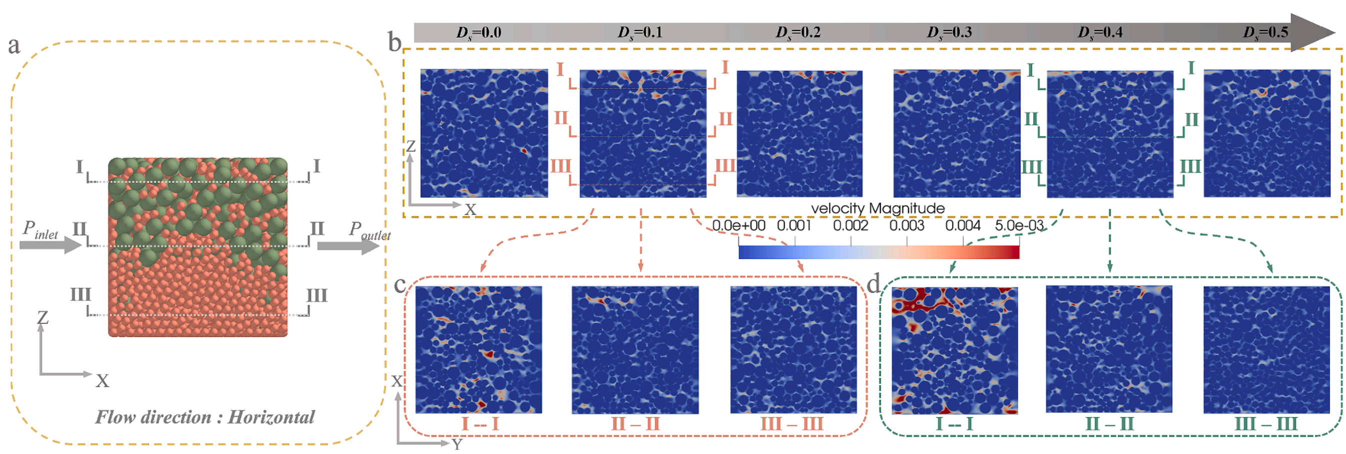

Fig. 17. (a) Schematic diagram of horizontal flow, (b) evolution of the velocity profile at the centre section with the degree of segregation, (c) velocity profile with D_s = 0.1, and (d) velocity profile with D_s = 0.4.

Geometry tortuosity.

Geometric tortuosity can be considered as a microscopic structural feature as it is determined by the geometric and morphological attributes of the porous media (Zhang et al. 2020). Various image analysis methods have been developed to evaluate the geometric tortuosity of digital microstructures of porous media, such as the Direct Shortest Path Search Method (DSPSM) (Stenzel et al. 2016), and Pore Centre Method (PCM) (Kaczmarek et al. 2017). These image-based methods directly operate on pixel/voxel data, making them generally easy to implement and computationally efficient. In this study, a numerical algorithm known as the Path Tracking Method (PTM) is employed to compute the geometric tortuosity of the granular system, particularly suitable for spherical-packed media (Sobieski et al. 2018; Sobieski and Lipiński 2019). The algorithm can identify the shortest paths in a given direction starting from a specified position. It calculates geometric tortuosity ($T_g = L/L_0$) as the ratio of the actual path length (L) of the space to the straight-line path length (L_0), which corresponds to the height of the sample. In this study, the bottom surface of the particle bed is divided into a regular grid of initial starting points (100 × 100). Subsequently, the lengths of 10,000 paths are calculated, and the average length is used to compute the geometric tortuosity of the porous media. As illustrated in Fig. 18, the plots of geometric tortuosity for selected cases (Fig. 18 a ~ b) indicate variations depending on the starting point of the path. Notably, regions with the same geometric tortuosity value are distinctly visible, as paths starting from nearby points often traverse the same or partially the same pore channels (Fig. 18 c).

Hydraulic tortuosity.

Contrary to geometric tortuosity, which characterises the microstructure of pores, hydraulic tortuosity focuses on the transport processes occurring within the microstructure. Numerical simulations of porous media can be performed to model various transport phenomena at the pore scale, thereby calculating the corresponding hydraulic tortuosity. The flow flux within porous media exhibits continuous variation along the flow path, influenced by factors such as cross-sectional area, shape, orientation, and branching. This complexity results in intricate pore-scale flow dynamics. As depicted in Fig. 19, local flow paths with relatively high velocities are clearly observed. Under similar conditions, material transport tends to occur through straighter and faster channels. In comparison with geometric tortuosity, hydraulic tortuosity can be influenced by preferential flows. In this study, the hydraulic tortuosity (T_h) is calculated using the vector-based tortuosity method (VTM), as introduced by Duda et al. (2011). This method is widely employed for evaluating hydraulic tortuosity, expressed as:

$$T_h = \frac{\int v(r)d\Omega}{\int v_x(r)d\Omega} = \frac{\langle V \rangle}{\langle V_x \rangle} \quad (16)$$

where $v_x(r)$ represents the velocity component parallel to the macroscopic flow direction at point r, and $\langle \ldots \rangle$ is a spatial average over the

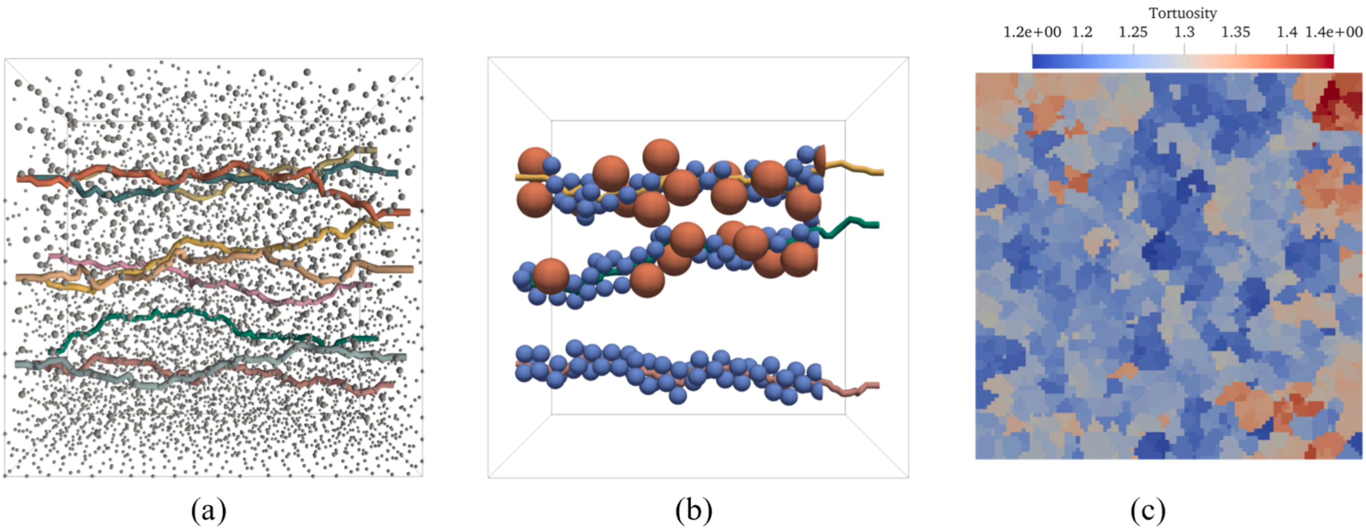

Fig. 18. Geometric tortuosity in porous media: (a) highlighted geometric path, with particles depicted in a reduced size; (b) geometric paths and the particles they pass through; (c) geometric tortuosity within a 100 × 100 grid.

pore space Ω. The hydraulic tortuosity is determined from the steady-state fluid velocity field.

In the previous sections, we demonstrated the seepage anisotropy induced by particle segregation, showcasing the evolution of complex pore structures and permeability. In this section, utilising the previously outlined tortuosity calculation methods, tortuosity for granular systems with different degrees of segregation is computed. Fig. 20(a) displays the obtained vertical and horizontal tortuosity values. The results indicate that tortuosity varies with the particle structure. In the initially uniformly mixed granular system, vertical and horizontal tortuosities exhibit similar values. However, as the granular system undergoes continuous segregation, a notable difference in tortuosity between different directions occurs, with horizontal tortuosity decreasing more significantly than vertical tortuosity. Consistent with prior research (Ghanbarian et al. 2013), hydraulic tortuosity is larger than geometric tortuosity, highlighting the complexity of material transport.

As a quantifiable index reflecting the complexity of pore structures, tortuosity is closely related to the permeability characteristics of porous media. Early studies found a positive relationship between tortuosity and porosity, leading to the establishment of a series of mathematical expressions relating porosity and tortuosity (Song et al. 2022; Zhang et al. 2020). Fig. 20(b) illustrates a comparison of results from several studies (Abderrahmene et al. 2017; Comiti and Renaud 1989; Dai et al. 2021; Millington 1959; Zhang et al. 2020). While these expressions provide straightforward representations of tortuosity that moderately align with experimental results, they overlook the impact of pore structure induced by particle arrangement on tortuosity. Consequently, there are variations in tortuosity expression results across different literature. In reality, the spatial arrangement of soil particles is highly complex. Changes in particle arrangement, even at the same porosity, have a significant impact on tortuosity. Particle segregation is a typical example of such particle rearrangement.

7. Conclusions

In this study, a numerical analysis framework is established to investigate the complex dynamic behaviour during particle segregation and assess its impact on pore structure, flow properties, and tortuosity of the porous media. The conclusions drawn from this research are as follows:

The study reveals a continuous evolution process from a uniformly mixed state to Brazil Nut segregation states. Detailed analysis of particle distribution and energy evolution explains the mechanisms of this phenomenon. The granular system does not achieve complete

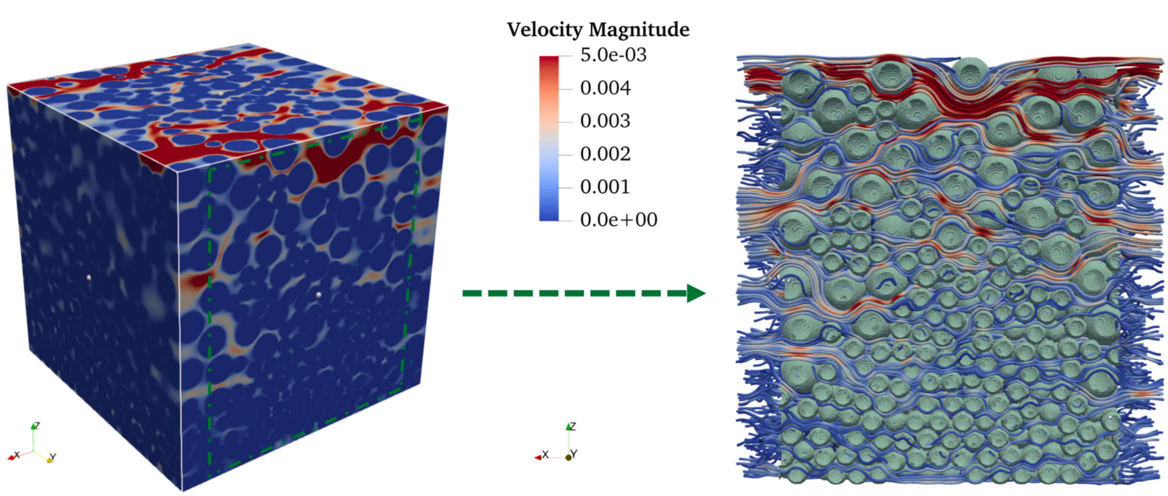

Fig. 19. Flow paths in porous media.

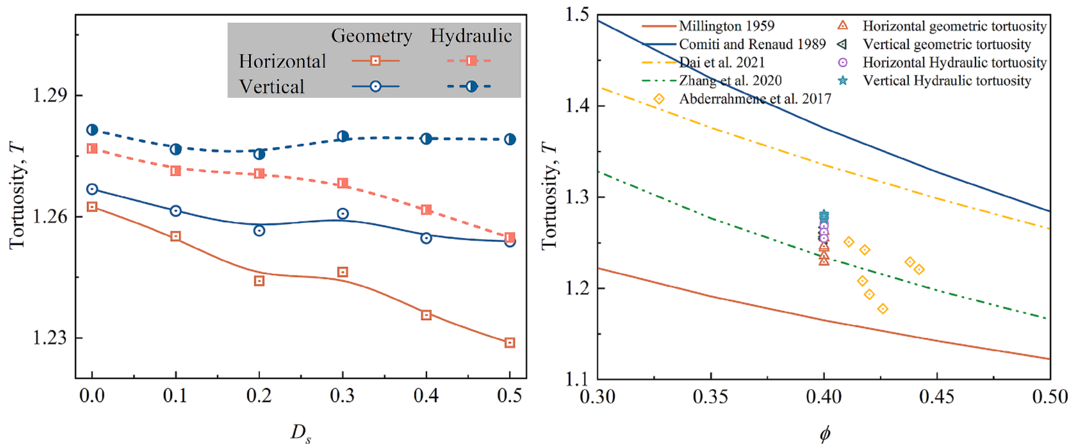

Fig. 20. (a) Tortuosity at different degrees of segregation, and (b) comparison of results on tortuosity.

segregation (final $D_s = 0.52$), with large particles segregating faster. Segregation primarily occurs when the granular material contacts the base, where a significant energy difference between large and small particles is observed.

Statistical analysis of the pore structure shows that pore diameters follow a lognormal distribution, with an average diameter of about 1 mm. In contrast, throat diameters exhibit a bimodal distribution, and sphericity follows a trimodal distribution with a distinct main peak. Segregation primarily affects local changes, with minimal impact on the overall distribution of pore structure. As segregation progresses, in the top layer, the accumulation of large particles reduces the pore count and increases sphericity. Conversely, in the bottom layer, the aggregation of small particles increases the pore count and decreases sphericity. The middle layer serves as an intermediate state. These changes present challenges for accurately predicting flow properties.

Particle segregation significantly affects flow properties, resulting in notable changes in permeability and velocity distribution. The aggregation of large particles in the upper part of the system increases horizontal permeability, while the accumulation of small particles in the lower part slightly decreases vertical permeability. The anisotropy induced by particle segregation adds complexity to predicting fluid flow in the pore space. A detailed comparative analysis of geometric and hydraulic tortuosity reveals that particle segregation reduces horizontal tortuosity while vertical tortuosity changes minimally.

The findings of the study contribute to a fundamental understanding of the Brazil Nut effect, providing insights into the evolution of pore structure and flow properties. The implications of this research are broad, covering multiple domains, including separation, filtration, petroleum recovery, and soil pollution migration. In these fields, where the dynamics of granular materials play a pivotal role in fluid transport, the outcomes of this investigation provide potential applications.

CRediT authorship contribution statement

Shaoheng Dai: Writing – original draft, Methodology, Investigation, Conceptualization. **Feng Shan:** Writing – review & editing, Validation. **Haibin Xiong:** Validation, Software. **Sheng Zhang:** Writing – review & editing, Project administration. **Xuzhen He:** Writing – review & editing, Supervision, Project administration. **Daichao Sheng:** Writing – review & editing, Supervision, Project administration.

Declaration of competing interest

The authors declare that they have no known competing financial interests or personal relationships that could have appeared to influence the work reported in this paper.

Acknowledgements

This research was supported by the Australian Research Council (https://www.arc.gov.au/) Discovery Early Career Researcher Award (DECRA; DE220100763), and the science and technology innovation Program of Hunan Province (2023RC1017). The authors would also like to express their gratitude to the anonymous reviewers for their insightful and valuable comments.

Data availability

Data will be made available on request.

References

Abderrahmene, M., AbdelIllah, B., Fouad, G., 2017. Electrical prediction of tortuosity in porous media. Energy Procedia 139, 718–724. https://doi.org/10.1016/j.egypro.2017.11.277.

Amirifar, R., Dong, K., Zeng, Q., An, X., Yu, A., 2021. Effect of vibration mode on self-assembly of granular spheres under three-dimensional vibration. Powder Technology 380, 47–58. https://doi.org/10.1016/j.powtec.2020.11.036.

Bakhshian, S., Hosseini, S.A., Shokri, N., 2019. Pore-scale characteristics of multiphase flow in heterogeneous porous media using the lattice Boltzmann method. Sci Rep 9 (1), 3377. https://doi.org/10.1038/s41598-019-39741-x.

Bertels, D., Willems, P., 2023. Physics-informed machine learning method for modelling transport of a conservative pollutant in surface water systems. Journal of Hydrology 619, 129354. https://doi.org/10.1016/j.jhydrol.2023.129354.

Bi, Y., He, S., Li, X., Ouyang, C., Wu, Y., 2016. Effects of segregation in binary granular mixture avalanches down inclined chutes impinging on defending structures. Environ Earth Sci 75 (3), 263. https://doi.org/10.1007/s12665-015-5076-1.

Brandao, R.J., Lima, R.M., Santos, R.L., Duarte, C.R., Barrozo, M.A.S., 2020. Experimental study and DEM analysis of granular segregation in a rotating drum. Powder Technology 364, 1–12. https://doi.org/10.1016/j.powtec.2020.01.036.

Bui, H.H., Nguyen, G.D., 2021. Smoothed particle hydrodynamics (SPH) and its applications in geomechanics: From solid fracture to granular behaviour and multiphase flows in porous media. Computers and Geotechnics 138, 104315. https://doi.org/10.1016/j.compgeo.2021.104315.

Carman, P.C., 1956. Flow of Gases Through Porous Media. Butterworths Scientific Publications, London.

Chen, F., Jiang, S., Xiong, H., Yin, Z., Chen, X., 2023. Micro pore analysis of suffusion in filter layer using tri-layer CFD–DEM model. Computers and Geotechnics 156, 105303. https://doi.org/10.1016/j.compgeo.2023.105303.

Chen, L., Šimůnek, J., Bradford, S.A., Ajami, H., Meles, M.B., 2024. Coupling water, solute, and sediment transport into a new computationally efficient hydrologic model. Journal of Hydrology 628, 130495. https://doi.org/10.1016/j.jhydrol.2023.130495.

Comiti, J., Renaud, M., 1989. A new model for determining mean structure parameters of fixed beds from pressure drop measurements: application to beds packed with parallelepipedal particles. Chemical Engineering Science 44 (7), 1539–1545. https://doi.org/10.1016/0009-2509(89)80031-4.

Cui, K.F.E., Zhou, G.G.D., Jing, L., 2021. "Viscous Effects on the Particle Size Segregation in Geophysical Mass Flows: Insights From Immersed Granular Shear Flow Simulations". JGR. Solid Earth 126 (8), e2021JB022274. https://doi.org/10.1029/2021JB022274.

Cundall, P.A., Strack, O.D.L., 1979. A discrete numerical model for granular assemblies. Géotechnique 29 (1), 47–65. https://doi.org/10.1680/geot.1979.29.1.47.

Dai, S., C. Tong, H. Yan, J. Teng, and S. Zhang. 2021. “Calculation of soil tortuosity based on sampling reliability.” Rock and Soil Mechanics, 42 (3): 855–862. https://doi.org/DOI: 10.16285/j.rsm.2020.0956.

Dai, S., X. He, C. Tong, F. Gao, S. Zhang, and D. Sheng. 2023. “Stability of sandy soils against internal erosion under cyclic loading and quantitatively examination of the composition and origin of eroded particles.” Can. Geotech. J., cgj-2023-0325. https://doi.org/10.1139/cgj-2023-0325.

Dai, B., Wu, F., Zhong, W., Shi, Y., Qin, J., Yang, J., Yang, J., 2022. Particle Sorting in Scree Slopes: Characterization and Interpretation From the Micromechanical Perspective. JGR Earth Surface 127 (5). https://doi.org/10.1029/2021JF006372.

Dai, S., Zhang, S., Gao, F., He, X., Sheng, D., 2024. Investigation of particle segregation in a vertically vibrated binary mixture: Segregation process and mechanism. Computers and Geotechnics 169, 106236. https://doi.org/10.1016/j.compgeo.2024.106236.

Ding, W.-T., Xu, W.-J., 2018. Study on the multiphase fluid-solid interaction in granular materials based on an LBM-DEM coupled method. Powder Technology 335, 301–314. https://doi.org/10.1016/j.powtec.2018.05.006.

Duda, A., Koza, Z., Matyka, M., 2011. Hydraulic tortuosity in arbitrary porous media flow. Phys. Rev. E 84 (3), 036319. https://doi.org/10.1103/PhysRevE.84.036319.

El-Sekelly, W., Abdoun, T., Dobry, R., 2016. Liquefaction Resistance of a Silty Sand Deposit Subjected to Preshaking Followed by Extensive Liquefaction. J. Geotech. Geoenviron. Eng. 142 (4), 04015101. https://doi.org/10.1061/(ASCE)GT.1943-5606.0001444.

Eshghinejadfard, A., Daróczy, L., Janiga, G., Thévenin, D., 2016. Calculation of the permeability in porous media using the lattice Boltzmann method. International Journal of Heat and Fluid Flow 62, 93–103. https://doi.org/10.1016/j.ijheatfluidflow.2016.05.010.

Feng, S.-J., Chen, J.-N., Chen, H.-X., Liu, X., Zhao, T., Zhou, A., 2020a. Analysis of sand – woven geotextile interface shear behavior using discrete element method (DEM). Can. Geotech. J. 57 (3), 433–447. https://doi.org/10.1139/cgj-2018-0703.

Feng, X., Zeng, J., Zhan, H., Hu, Q., Ma, Z., Feng, S., 2020b. Resolution effect on image-based conventional and tight sandstone pore space reconstructions: Origins and strategies. Journal of Hydrology 586, 124856. https://doi.org/10.1016/j.jhydrol.2020.124856.

Fu, J., Thomas, H.R., Li, C., 2021. Tortuosity of porous media: Image analysis and physical simulation. Earth-Science Reviews 212, 103439. https://doi.org/10.1016/j.earscirev.2020.103439.

Gao, F., Zhang, S., He, X., Sheng, D., 2022. Experimental Study on Migration Behavior of Sandy Silt under Cyclic Load. J. Geotech. Geoenviron. Eng. 148 (5), 06022003. https://doi.org/10.1061/(ASCE)GT.1943-5606.0002796.

Ghanbarian, B., Hunt, A.G., Ewing, R.P., Sahimi, M., 2013. Tortuosity in Porous Media: A Critical Review. Soil Science Society of America Journal 77 (5), 1461–1477. https://doi.org/10.2136/sssaj2012.0435.

Gostick, J.T., 2017. Versatile and efficient pore network extraction method using marker-based watershed segmentation. Phys. Rev. E 96 (2), 023307. https://doi.org/10.1103/PhysRevE.96.023307.

Guo, N., Zhao, J., 2013. The signature of shear-induced anisotropy in granular media. Computers and Geotechnics 47, 1–15. https://doi.org/10.1016/j.compgeo.2012.07.002.

Hazzar, L., Nuth, M., Chekired, M., 2020. DEM simulation of drained triaxial tests for glass-beads. Powder Technology 364, 123–134. https://doi.org/10.1016/j.powtec.2019.09.095.

He, X., Liang, D., Bolton, M.D., 2018. Run-out of cut-slope landslides: mesh-free simulations. Géotechnique 68 (1), 50–63. https://doi.org/10.1680/jgeot.16.P.221.

He, X., Wu, W., Wang, S., 2019a. A constitutive model for granular materials with evolving contact structure and contact forces—Part I: framework. Granular Matter 21 (2), 16. https://doi.org/10.1007/s10035-019-0868-8.

He, X., Wu, W., Wang, S., 2019b. A constitutive model for granular materials with evolving contact structure and contact forces—part II: constitutive equations. Granular Matter 21 (2), 20. https://doi.org/10.1007/s10035-019-0869-7.

He, X., Wu, W., Cai, G., Qi, J., Kim, J.R., Zhang, D., Jiang, M., 2020. Work–energy analysis of granular assemblies validates and calibrates a constitutive model. Granular Matter 22 (1), 28. https://doi.org/10.1007/s10035-019-0990-7.

Hertz, H., 1882. On the contact of elastic solids. J Reine Angew Math 92, 156–171.

Indraratna, B., Phan, N.M., Nguyen, T.T., Huang, J., 2021. Simulating Subgrade Soil Fluidization Using LBM-DEM Coupling. Int. J. Geomech. 21 (5), 04021039. https://doi.org/10.1061/(ASCE)GM.1943-5622.0001997.

Ishiyama, K., Yamamoto, K., Harada, S., Yagi, T., 2023. Tortuosity of Internal Pore Space in Variously Structured Platelet Particles. Transp Porous Med 148 (3), 535–557. https://doi.org/10.1007/s11242-023-01958-w.

Kaczmarek, Ł.D., Zhao, Y., Konietzky, H., Wejrzanowski, T., Maksimczuk, M., 2017. Numerical Approach in Recognition of Selected Features of Rock Structure from Hybrid Hydrocarbon Reservoir Samples Based on Microtomography. Studia Geotechnica et Mechanica 39 (1), 13–26. https://doi.org/10.1515/sgem-2017-0002.

Kozeny, J. 1927. “Uber kapillare leitung des wassers im boden.” Sitzungsberichte der Kaiserlichen Akademie der Wissenschaften, 2a (136): 271–306.

Latt, J., Malaspinas, O., Kontaxakis, D., Parmigiani, A., Lagrava, D., Brogi, F., Belgacem, M.B., Thorimbert, Y., Leclaire, S., Li, S., Marson, F., Lemus, J., Kotsalos, C., Conradin, R., Coreixas, C., Petkantchin, R., Raynaud, F., Beny, J., Chopard, B., 2021. Palabos: Parallel Lattice Boltzmann Solver. Computers & Mathematics with Applications 81, 334–350. https://doi.org/10.1016/j.camwa.2020.03.022.

Li, G., Wang, D., Liu, Q., Zhao, Y., Duan, C., 2022. Separation performance of 0.5–1 mm fine coal in a gas–solid fluidized bed without dense medium. Fuel 318, 123645. https://doi.org/10.1016/j.fuel.2022.123645.

Lindquist, W.B., Lee, S., Coker, D.A., Jones, K.W., Spanne, P., 1996. Medial axis analysis of void structure in three-dimensional tomographic images of porous media. J. Geophys. Res. 101 (B4), 8297–8310. https://doi.org/10.1029/95JB03039.

Liu, S., Hu, W., Gong, J., Nie, Z., 2022. An improved index of mixing degree and its effect on the strength of binary geotechnical mixtures. Granular Matter 24 (1), 6. https://doi.org/10.1007/s10035-021-01168-5.

Liu, C., Zhao, Y., Li, Y., Feng, Y., Duan, C., Zhou, C., Dong, L., 2024. A model for predicting the segregation directions of binary Geldart B particle mixtures in bubbling fluidized beds. Particuology 90, 340–349. https://doi.org/10.1016/j.partic.2024.01.006.

Masís-Meléndez, F., Chamindu Deepagoda, T.K.K., De Jonge, L.W., Tuller, M., Moldrup, P., 2014. Gas diffusion-derived tortuosity governs saturated hydraulic conductivity in sandy soils. Journal of Hydrology 512, 388–396. https://doi.org/10.1016/j.jhydrol.2014.02.063.

Metzger, M.J., Remy, B., Glasser, B.J., 2011. All the Brazil nuts are not on top: Vibration induced granular size segregation of binary, ternary and multi-sized mixtures. Powder Technology 205 (1–3), 42–51. https://doi.org/10.1016/j.powtec.2010.08.062.

Millington, R.J., 1959. Gas Diffusion in Porous Media. Science, New Series 130 (3367), 100–102.

Mindlin, R.D., 1949. Compliance of Elastic Bodies in Contact. JOURNAL OF APPLIED MECHANICS.

Muresan, B., Saiyouri, N., Guefrech, A., Hicher, P.-Y., 2011. Internal erosion of chemically reinforced granular materials: A granulometric approach. Journal of Hydrology 411 (3–4), 178–184. https://doi.org/10.1016/j.jhydrol.2011.09.009.

Nguyen, H.B.K., Rahman, M.M., Fourie, A., 2021. The critical state behaviour of granular material in triaxial and direct simple shear condition: A DEM approach. Computers and Geotechnics 138, 104325. https://doi.org/10.1016/j.compgeo.2021.104325.

Nie, Y., Wang, X., 2024. Impact of sediment uniformity from steep tributary on transport in main Channels: A CFD-DEM study. Journal of Hydrology 640, 131688. https://doi.org/10.1016/j.jhydrol.2024.131688.

Panda, S., Tan, D.S., 2020. Effect of external factors on segregation of different granular mixtures. Advanced Powder Technology 31 (2), 571–594. https://doi.org/10.1016/j.apt.2019.11.013.

Qiao, J., Duan, C., Dong, K., Wang, W., Jiang, H., Zhu, H., Zhao, Y., 2021. DEM study of segregation degree and velocity of binary granular mixtures subject to vibration. Powder Technology 382, 107–117. https://doi.org/10.1016/j.powtec.2020.12.064.

Qiu, W., Li, Y., Zhang, Y., Wen, L., Wang, T., Wang, J., Sun, X., 2024. Numerical investigation on the evolution process of cascade dam-break flood in the downstream earth-rock dam reservoir area based on coupled CFD-DEM. Journal of Hydrology 635, 131162. https://doi.org/10.1016/j.jhydrol.2024.131162.

Ren, X.W., Santamarina, J.C., 2018. The hydraulic conductivity of sediments: A pore size perspective. Engineering Geology 233, 48–54. https://doi.org/10.1016/j.enggeo.2017.11.022.

Sangani, A.S., Acrivos, A., 1982. Slow flow through a periodic array of spheres. International Journal of Multiphase Flow 8 (4), 343–360. https://doi.org/10.1016/0301-9322(82)90047-7.

Siman-Tov, S., Brodsky, E.E., 2018. Gravity-Independent Grain Size Segregation in Experimental Granular Shear Flows as a Mechanism of Layer Formation. Geophys. Res. Lett. 45 (16), 8136–8144. https://doi.org/10.1029/2018GL078486.

Sobieski, W., Lipiński, S., 2019. The influence of particle size distribution on parameters characterizing the spatial structure of porous beds. Granular Matter 21 (2), 14. https://doi.org/10.1007/s10035-019-0866-x.

Sobieski, W., Matyka, M., Gołembiewski, J., Lipiński, S., 2018. The Path Tracking Method as an alternative for tortuosity determination in granular beds. Granular Matter 20 (4), 72. https://doi.org/10.1007/s10035-018-0842-x.

Song, S., Rong, L., Dong, K., Shen, Y., 2022. Numerical study of the hydraulic tortuosity for fluid flow through elliptical particle packings. Powder Technology 398, 117047. https://doi.org/10.1016/j.powtec.2021.117047.

Stenzel, O., Pecho, O., Holzer, L., Neumann, M., Schmidt, V., 2016. Predicting effective conductivities based on geometric microstructure characteristics. AIChE Journal 62 (5), 1834–1843. https://doi.org/10.1002/aic.15160.

Stipić, D., Budinski, L., Fabian, J., 2022. Sediment transport and morphological changes in shallow flows modelled with the lattice Boltzmann method. Journal of Hydrology 606, 127472. https://doi.org/10.1016/j.jhydrol.2022.127472.

To, P., Agius, D., Cussen, L., 2020. Influence of relative density of the granular base soil on filter performance. Acta Geotech. 15 (12), 3621–3627. https://doi.org/10.1007/s11440-020-01064-x.

To, H. D., Scheuermann, Alexander, and Williams, David J. (2012). “A new simple model for the determination of the pore constriction size distribution.” Paris, Franc: Paris, France: Société Hydrotechnique de France (SHF).

To, H.D., Galindo-Torres, S.A., Scheuermann, A., 2016a. Sequential sphere packing by trilateration equations. Granular Matter 18 (3), 70. https://doi.org/10.1007/s10035-016-0666-5.

To, H.D., Scheuermann, A., Galindo-Torres, S.A., 2016b. Probability of Transportation of Loose Particles in Suffusion Assessment by Self-Filtration Criteria. J. Geotech. Geoenviron. Eng. 142 (2), 04015078. https://doi.org/10.1061/(ASCE)GT.1943-5606.0001403.

To, P., Scheuermann, A., Williams, D.J., 2018. Quick assessment on susceptibility to suffusion of continuously graded soils by curvature of particle size distribution. Acta Geotech. 13 (5), 1241–1248. https://doi.org/10.1007/s11440-017-0611-8.

Wang, R., Fu, P., Zhang, J.-M., Dafalias, Y.F., 2019. Fabric characteristics and processes influencing the liquefaction and re-liquefaction of sand. Soil Dynamics and Earthquake Engineering 125, 105720. https://doi.org/10.1016/j.soildyn.2019.105720.

Wang, J.-P., Liu, T.-H., Wang, S.-H., Luan, J.-Y., Dadda, A., 2023. Investigation of porosity variation on water retention behaviour of unsaturated granular media by using pore scale Micro-CT and lattice Boltzmann method. Journal of Hydrology 626, 130161. https://doi.org/10.1016/j.jhydrol.2023.130161.

Wu, M., Cheng, Z., Wu, J., Wu, J., 2017. Quantifying representative elementary volume of connectivity for translucent granular materials by light transmission micro-tomography. Journal of Hydrology 545, 12–27. https://doi.org/10.1016/j.jhydrol.2016.11.063.

Wu, M., Wu, J., Wu, J., Hu, B.X., 2018. A three-dimensional model for quantification of the representative elementary volume of tortuosity in granular porous media. Journal of Hydrology 557, 128–136. https://doi.org/10.1016/j.jhydrol.2017.12.030.

Xiong, Y., Dong, L., Long, X., Chen, M., Huang, G., 2022. Pore-network model to quantify internal structure and hydraulic characteristics of randomly packed grains with different morphologies. Granular Matter 24 (1), 10. https://doi.org/10.1007/s10035-021-01174-7.

Yamamoto, K., Ishiyama, K., Harada, S., 2023. Quantitative Evaluation of the Pore Characteristics in Platelet Particle Beds by Pore Network Modeling. Transp Porous Med 150 (1), 89–108. https://doi.org/10.1007/s11242-023-01997-3.

Yang, G.C., Jing, L., Kwok, C.Y., Sobral, Y.D., 2019. A comprehensive parametric study of LBM-DEM for immersed granular flows. Computers and Geotechnics 114, 103100. https://doi.org/10.1016/j.compgeo.2019.103100.

Yin, P., Song, H., Ma, H., Yang, W., He, Z., Zhu, X., 2022. The modification of the Kozeny-Carman equation through the lattice Boltzmann simulation and experimental verification. Journal of Hydrology 609, 127738. https://doi.org/10.1016/j.jhydrol.2022.127738.

Younes, N., Wautier, A., Wan, R., Millet, O., Nicot, F., Bouchard, R., 2023. DEM-LBM coupling for partially saturated granular assemblies. Computers and Geotechnics 162, 105677. https://doi.org/10.1016/j.compgeo.2023.105677.

Zhang, S., Yan, H., Teng, J., Sheng, D., 2020. A mathematical model of tortuosity in soil considering particle arrangement. Vadose Zone J. 19 (1). https://doi.org/10.1002/vzj2.20004.

Zhang, Z., Zhang, Z., Lu, W., Guo, H., Liu, C., Ning, F., 2024. Pore-scale investigations of permeability of saturated porous media: Pore structure efficiency. Journal of Hydrology 637, 131441. https://doi.org/10.1016/j.jhydrol.2024.131441.

Zhao, J., Qin, F., Derome, D., Carmeliet, J., 2020. Simulation of quasi-static drainage displacement in porous media on pore-scale: Coupling lattice Boltzmann method and pore network model. Journal of Hydrology 588, 125080. https://doi.org/10.1016/j.jhydrol.2020.125080.